INTERNATIONAL JOURNAL FOR NUMERICAL METHODS IN FLUIDS, VOL. 16, 353–364 (1993)

STRATIFIED FLOW UNDER AN ICE KEEL— A NUMERICAL APPROACH

M. I. JAMEEL AND R. D. ROWE

Department of Mechanical Engineering, The University of Calgary, Calgary, Alberta, Canada T2N 1N4

AND

D. R. TOPHAM

Institute of Ocean Sciences, 9860 West Saanich Road, Sydney, BC, Canada V8L 4B2

SUMMARY

A numerical investigation of the flow of two immiscible stratified fluids under an isolated keel has been undertaken. The investigation utilized the two-dimensional Euler equations for incompressible flow, and the solution of these equations has been obtained by using the well-known finite volume marker and cell approach. Experimental drag-force measurements are also presented for a family of two-dimensional topographic models of fixed height with increasing surface slopes in a two-layer density system. The range of flow speeds explored covers the Froude number range from subcritical to fully supercritical. The drag force measurements are augmented by detailed observations of the interface distortion. The results clearly show large drag increases arising from the internal wave systems generated in the stratified flow. Very good agreement has been found between the experimental and numerical results for both the interface shape between the two fluids and the drag force on a variety of keels.

KEY WORDS Ice keels Drag Stratified flow Marker and cell SOLA-VOF

INTRODUCTION

In the spring of 1985, D. R. Topham and his colleagues at the Institute of Ocean Sciences (Sydney, British Columbia) conducted a field study of flow under an isolated ice keel at the Barrow Strait in the Beaufort Sea. This experiment was aimed at understanding the interaction of the Arctic ice pack with the underlying ocean in order to estimate the drag force between them. From the field observations, it has been found that the Arctic Ocean is stratified in two distinct layers of water at this location. The stratification is determined by the salinity of the water and maintained by the melting of the ice pack.[1]

Based on the information gathered in the field, a laboratory experiment was set up at the Institute to look at the flow of two stably stratified fluids flowing under an isolated keel. To study this experimentally, an arrangement was devised to tow the keel in a channel containing the fluids (fresh and salt water). The keel was attached to a flat board that floated at the free surface of the upper fluid. In this study, the experiments were run for keels of the same maximum height but varying lengths; in fact a 'Witch of Agnesi' family of four two-dimensional topographic models of fixed height with increasing surface slopes were used. In addition to recording the interface shape between the two fluids, a measurement of the drag force was made for each keel (except for the

0271–2091/93/050353–12$11.00

Received December 1991
Revised September 1992

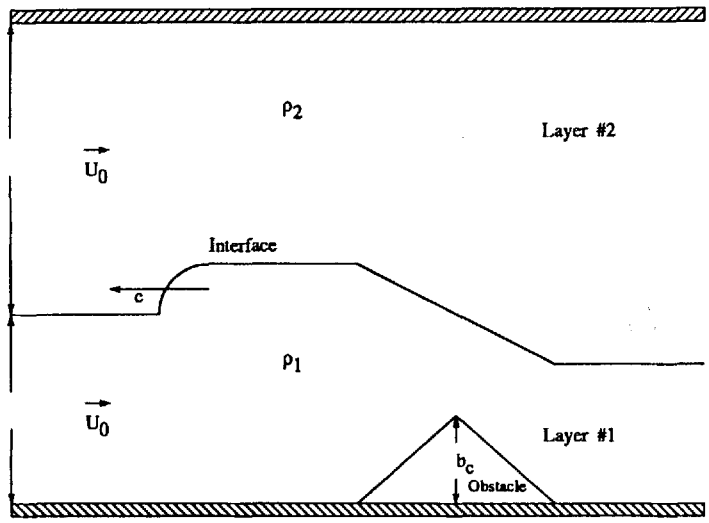

Figure 1. Schematic indicating the physical parameters for two-layer flow over an obstacle

longest keel) for selected values of the towing speed; a detailed account of this is provided in Reference 2.

Some of the early analytical and experimental investigations of this two-layer flow problem were conducted by Long.[3-5] In recent years, a comprehensive study of this problem has been carried out by Baines.[6] Baines proposed a classification scheme similar to that for single fluids given by Baines and Davies.[7] From these studies it can be concluded that the flow of two fluids over an isolated ridge is governed by the following dimensionless parameters:

$$F_0=\frac{u_0}{\sqrt{[(1-s)gh_0]}}, \quad B_c=\frac{b_c}{h_0}, \quad r=\frac{H}{h_0}, \quad s=\frac{\rho_2}{\rho_1}.$$

These flow parameters are illustrated in Figure 1.

Previous numerical investigations of this problem have been limited to simple hydraulic solutions. These solutions involved solving the shallow-water equations, i.e. flows with one-dimensional uniform velocities and hydrostatic-pressure distributions. A notable solution using this technique is that of Houghton and Isaacson.[8] A similar study for single-layer flow has been carried out by Houghton and Kasahara.[9]

NUMERICAL SOLUTION

The numerical investigation described in this paper utilizes the two-dimensional Euler equations for incompressible flow. The solution of these equations has been obtained by the well-known Marker And Cell (MAC) finite differencing scheme developed by Harlow and Welch.[10] One of the difficulties experienced in modelling such problems is the management of the free surface or fluid interface. This has been handled successfully by the introduction of a volume of fluid function, measured at the centre of each finite difference grid cell. Details of the solution technique can be found in the program manual for the SOLA-VOF (solution algorithm based on the fractional volume of fluid) code.[11] The need to implement such a code for a problem of this type is created by the requirement to keep track of a complex density interface. The technique uses a finite

differencing scheme which advances explicitly in time. It is worthwhile noting that the maximum Courant number allowed by the interface convection algorithm is one, so the explicit nature of the convection term calculation does not in fact limit the speed with which the solution can be obtained.

The numerical simulations reported here have been carried out at the University of Calgary in conjunction with laboratory experiments at the Institute of Ocean Sciences, Sydney, British Columbia. The laboratory experiment consists of an inverted keel shape being towed on the surface of a stable stratification of salt and fresh water, whereas the numerical model has been set up with the obstacle on the bottom of the flume with a rigid lid adjacent to the upper layer fluid as illustrated in Figure 1. This difference is of no consequence to the problem being examined here, as it is the internal dynamics of the flow that is relevant to the problem, e.g. Reference 6. The results selected for discussion in this paper are those for keel # 1, and a listing of the physical parameters for both the experimental and numerical models is given in Table I.

From a series of numerical runs, it was found that a grid cell whose dimensions are of the ratio $\delta y : \delta x \leqslant 1:2$ (δy and δx are the vertical and horizontal dimensions of a finite difference cell) yielded stable solutions. A major concern in any numerical simulation of this nature is the duration of the computer time. Computations were repeated for a finer grid, with no significant improvements in results. Therefore, to minimize computation time, the ratio $\delta y : \delta x = 1:2$ was used.

The numerical model consists of a finite difference mesh of 200 uniform grid cells ($\delta x = 2{\cdot}2$ cm) in the horizontal direction. In the vertical direction, the mesh is divided into two grid blocks. The first grid block is comprised of 10 uniform cells ($\delta y = 1{\cdot}1$ cm). This block makes up the region containing the lower fluid and the obstacle, which is also known as the active layer. Above it is a second block described by a non-uniform grid consisting of 20 cells with heights varying as follows: $1{\cdot}1 \text{ cm} \leqslant \delta y \leqslant 5{\cdot}0$ cm. This second block contains the upper fluid and is referred to as the passive layer. The interface region of these two grid blocks contains two rows of cells ($\delta y = 1{\cdot}1$ cm). This facilitates a smooth transition from the uniform to the non-uniform grid. The largest value of δy is situated at the furthest distance away from the two fluid interface, and in this region the velocity and pressure of the fluid did not change much from one time step to the next. Therefore, the large ratio of $\delta y : \delta x$ in this region did not pose a problem in convergence at any time step.

The ridge shape was generated by blocking off a combination of grid cells to approximate the shape of keels, as illustrated in Figure 2 for keel # 1. The base lengths of all four numerical keels are listed in Table II. The maximum height of all of the obstacles is 5·5 cm and, therefore, only 5 grid cells are blocked in the vertical direction. This arrangement was chosen so that the obstacle height would be half the depth of the first layer of fluid. Despite the jagged shape generated by this style of blocking, Hirt[12] proposed that the fluid actually 'sees' a shape close to that formed by the horizontal steps together with the diagonals depicted by the bold lines in Figure 2. Each diagonal

Table I. Physical parameters for the numerical and experimental models

Parameters	Numerical	Experimental
Density of fluid # 1 (g/cm^3)	1·02	1·02
Density of fluid # 2 (g/cm^3)	1·00	1·00
Depth of the fluid layer # 1 (cm)	11·00	11·00
Total depth for both fluids (cm)	70·00	70·00
Maximum obstacle height (cm)	5·50	5·50
Length of tank (cm)	440·00	1000·00

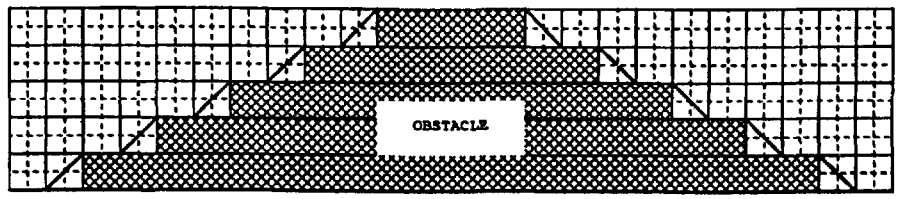

Figure 2. Illustration of the blocked off cells in the mesh. The bold diagonal lines indicate the final shape seen by the fluid (Reference 12)

Table II. Maximum keel lengths for the four keels. The lengths are measured at the base of the keels

Keel no.	Maximum keel length (cm)
1	44
2	66
3	88
4	176

in this figure passes through the centre point of that grid cell, where the pressure is determined. Thus, the drag force per unit width can easily be obtained by integrating the pressures along the surface of the obstacle.

The boundary conditions for this flow are constant, uniform inflow conditions at the left and outflow at the right. All boundary conditions at the floor and the ceiling are free slip, since the scales resolved in this problem are much greater than those of the viscous boundary layer. Initially, it is assumed that the interface between the two fluids is flat and horizontal and there is a uniform flow speed throughout both layers.

The gravity term in the two-fluid case is reduced by the factor $(1-s)$ and, therefore, the initial velocity needed to start the computations is significantly lower than that for the identical single-layer fluid flow problem with the same active layer depth. This translates into a relatively more slowly changing flow field than the one with only a single fluid; see, for example, Reference 13. Thus, in order to establish a reasonably quasi-steady flow, the computations had to be carried to a time t of at least 20 s.

INTERFACE RESULTS

The numerical runs were made for a variety of upstream Froude numbers F_0, ranging from 0·2 to 1·7 in 0·1 steps. These runs were conducted for a single value of $B_c = 0{\cdot}5$, $r = 70/11 = 6{\cdot}36$ and $s = 0{\cdot}98$. The interface shapes predicted by the numerical model for $F_0 = 0{\cdot}5$, 0·7, 1·0, 1·3 and 1·7 at times of 10 s and 20 s are shown in Figure 3. The interface shapes obtained from the laboratory experiments at $F_0 = 0{\cdot}54$, 0·71, 1·04, 1·27 and 1·68 are also displayed in this figure. The line identified as the 'theoretical profile' is the solution based on hydraulic theory, i.e. the fluid is assumed to have a single component of velocity (horizontal), which is uniform in the vertical direction, and the pressure distribution in the fluid is assumed to be hydrostatic. It can be seen that there is a very good match between the numerical model and the laboratory experiment for all of the Froude number cases.

When $F_0 = 0{\cdot}5$ (Figure 3(a)), a well-defined upstream bore is produced with a hydraulic control at the crest of the obstacle, as would be predicted by simple hydraulic theory. However, when $F_0 = 0{\cdot}7$ (Figure 3(b)), the upstream interface consists of a bulge that appears to be anchored at the crest of the obstacle and stretches laterally in the upstream direction with time. It is this type of behaviour that Houghton and Isaacson[8] and Baines[6] refer to as a rarefaction; this significant change in the type of upstream blocking does not occur in single-layer fluid flows. The computer program maintains the initial conditions at the outflow end of the grid in a manner similar to a weir with its associated hydraulic control. For this reason, the downstream flow deviates significantly from the experimentally observed supercritical jet for these subcritical flows.

For $F_0 = 1{\cdot}0$ (Figure 3(c)), the upstream blocking seen in the higher Froude number subcritical flows has diminished substantially. Instead, an almost symmetrical interface shape similar to that for supercritical flow at high Froude numbers is formed. It appears that an intermediate flow

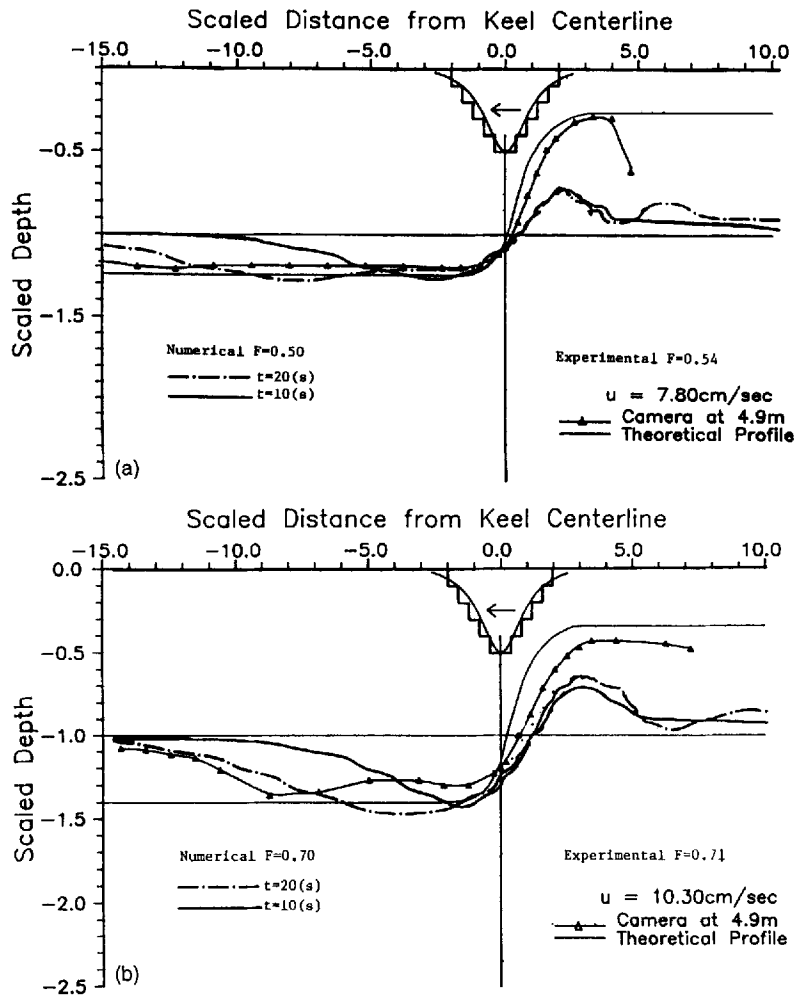

Figure 3. Comparison of the numerical and experimental interface shape between the two fluids for various Froude numbers. The theoretical profile is for a hydraulic type flow. The experimental data were obtained with a video camera at a fixed distance from the starting point. The results are for keel #1

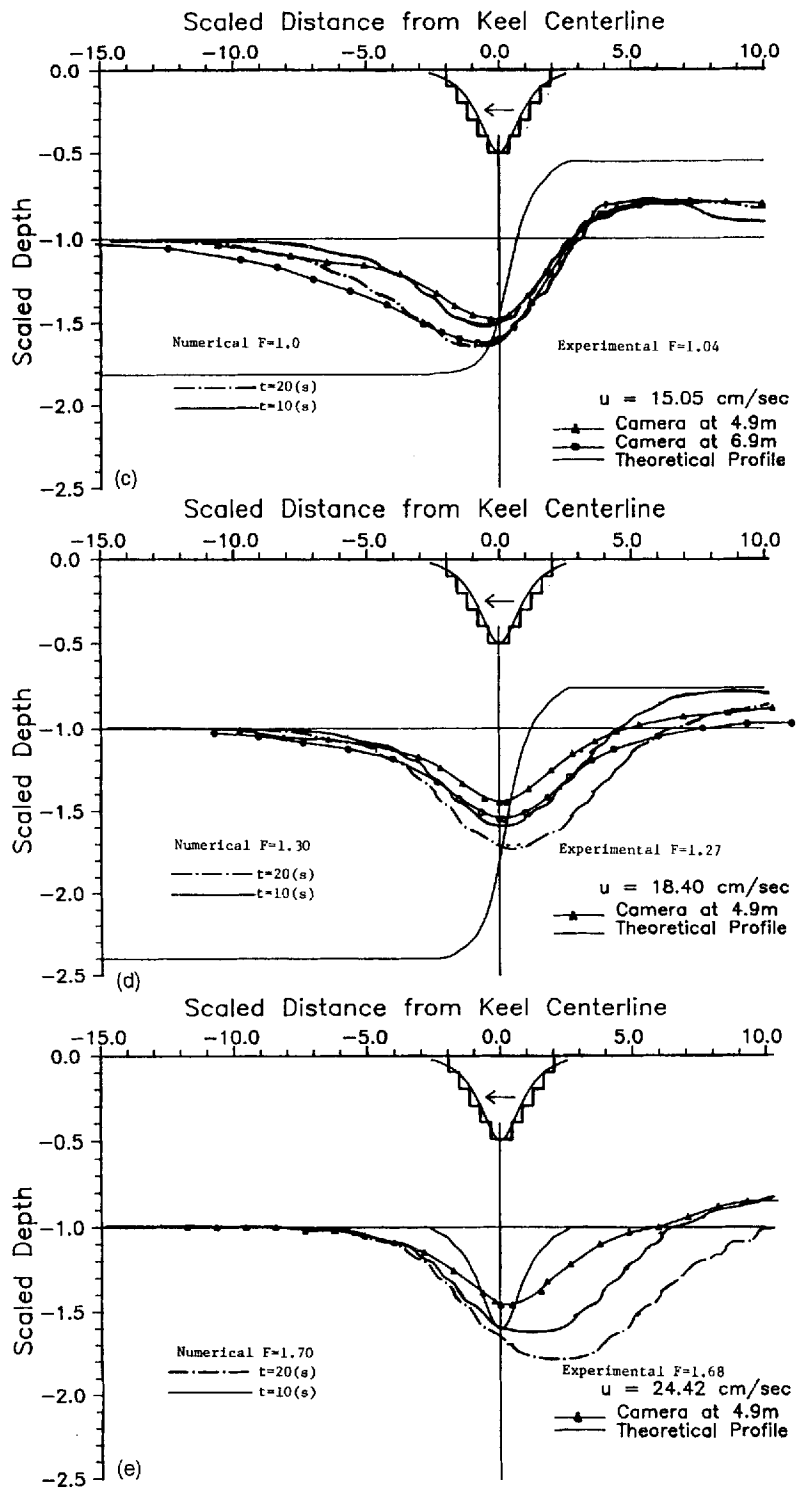

Figure 3. (Continued)

structure occurs in the lower Froude number supercritical flows that is distinctly two-dimensional in nature and cannot, therefore, be modelled by simple hydraulic theory. The simplest two-dimensional feature that could fit such a shape is a stationary solitary wave. Similar remarks apply for the $F_0 = 1{\cdot}3$ case as shown in Figure 3(d).

For supercritical flows with higher Froude number such as $F_0 = 1{\cdot}7$, it is seen in Figure 3(e) that a noticeable swelling of the interface occurs on the lee side of the obstacle. A closer look at this region of the flow shows the presence of a recirculation zone, as can be seen in the plot of the stream lines on the lee side of the keel in Figure 4. This recirculation bubble is also found to exist for slightly lower Froude numbers ($F_0 = 1{\cdot}5$ and $1{\cdot}6$). The appearance of such a two-dimensional flow feature could possibly be what Baines[6] had to model as a 'hydraulic drop', due to limitations of hydraulic theory. Surprisingly, the flow phenomenon computed here occurs with a free-slip boundary condition and with a grid size larger than the boundary layer thickness. Experimental observations reveal boundary layer separation close to the crest of the keel leading to a similar interface shape. The same type of results have been reported for a similar finite-volume numerical code by Hirt[14] for the flow of a continuous fluid over a backward facing step.

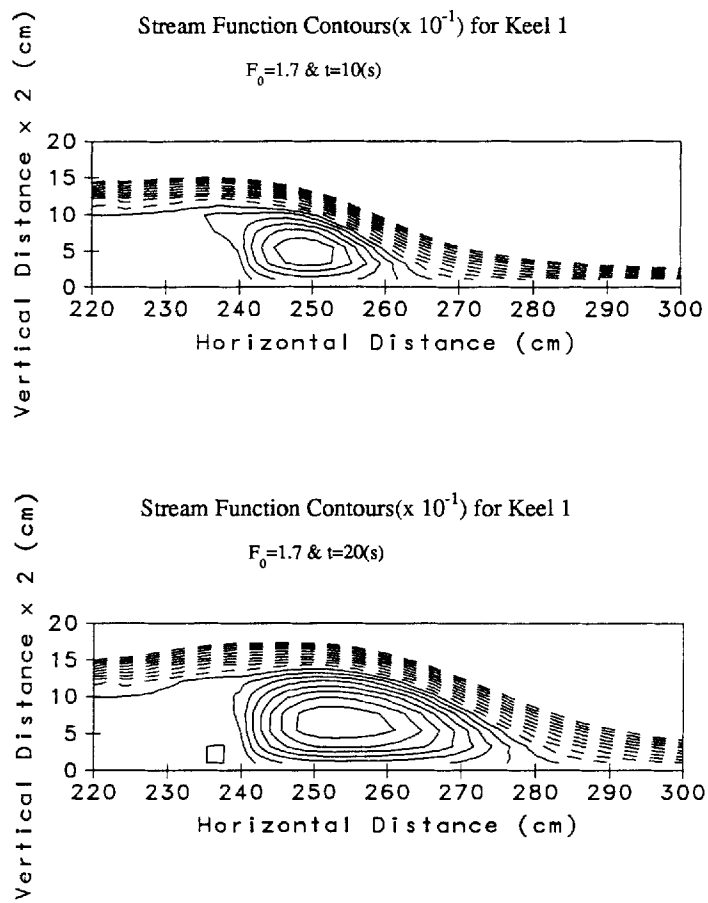

Figure 4. Plot of the stream-lines in the lower part of the active layer on the lee side of the keel. The centre of the keel is located 220 cm from the inlet section

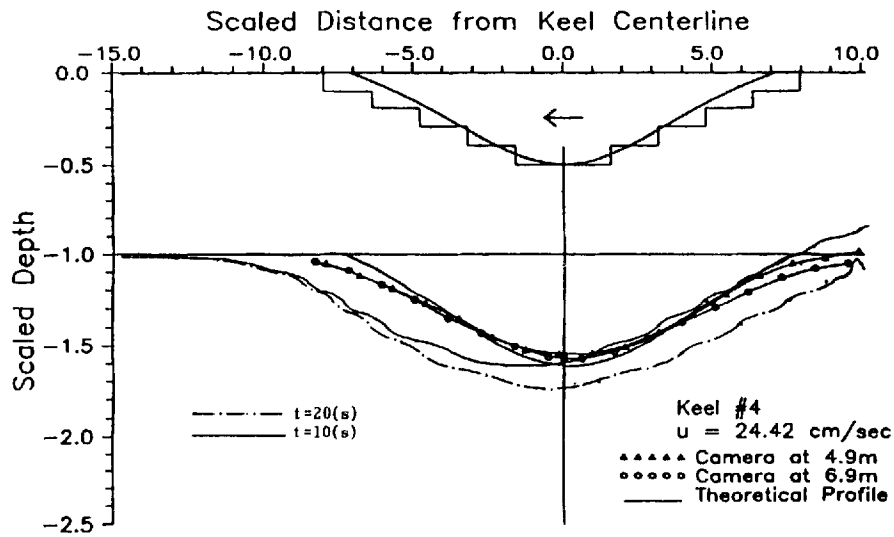

Figure 5. Comparison of the numerical and experimental interface shape between the two fluids for keel #4. The theoretical profile is for a hydraulic type flow. The experimental data were obtained with a video camera at a fixed distance from the starting point

In contrast to the flow behaviour over keel #1 (for $F_0 = 1{\cdot}7$), the longest obstacle, keel #4, produces an interface shape that is very close to that predicted by hydraulic theory, see Figure 5. This theory suggests that the shape of the interface over the obstacle should be in the form of a symmetrical hump for $F_0 = 1{\cdot}7$. It can be seen in Figure 5 that all three results (experimental data, hydraulic theory and numerical model) are in harmony. The lee side antisymmetric flow feature seen for keel #1 is not present. The lee side stream functions have also been computed for keel #4, and these results are plotted in Figure 6. It is seen that in this case the lee side vortex is totally absent. Naturally, one can conclude that it is the mild shape of keel #4 that leads to the difference in results.

DRAG RESULTS

The drag force experienced by the ridge has been calculated by integrating the pressure obtained from the numerical simulation along the ridge surface; the width of the keel is 30 cm. A comparison of these numerical results with the laboratory keel drag forces for keel #1 is provided in Figure 7. The experimental results are slightly higher than the numerical predictions. This is to be expected because the numerical model is only solving the Euler equations and, therefore, does not account for viscous forces.

The drag force rises to a maximum around $F_0 = 0{\cdot}7$ and then it falls with increasing Froude number. This relatively rapid drop in drag is due to the change in the type of upstream blocking as discussed in the previous section. Both the numerical and experimental results follow this trend until the flow is supercritical ($F_0 \sim 1{\cdot}1$), when once again the drag rises with increasing Froude number. Experimental observations reveal a separation of the boundary layer on the lee side of the obstacle at this point, while the numerical code gives rise to the development of a recirculation zone in response to the overshooting of the numerical velocity field beyond the crest of the obstacle. Surprisingly, these two models predict almost the same drag behaviour but for different

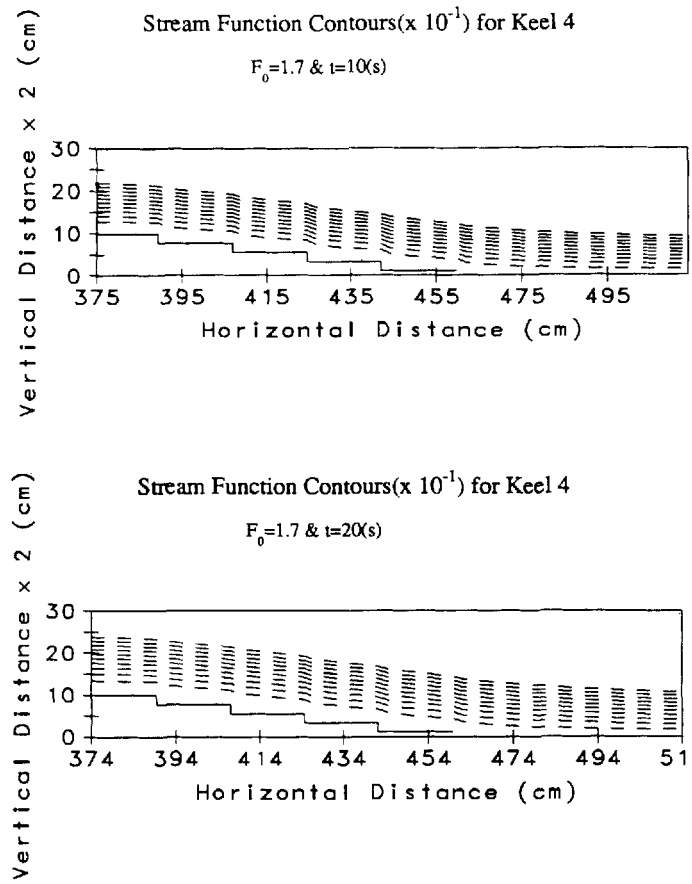

Figure 6. Plot of stream-lines in the lower part of the active layer on the lee side of the keel. The centre of the keel is located 374 cm from the inlet section

reasons. The net effect in either case is a similar elevation of the lee side interface as seen in Figure 3(e) for $F_0 = 1{\cdot}7$, which results in approximately the same increase in drag. This type of recirculation can never be identified in numerical schemes using the one-dimensional shallow-water equations, which can result in the prediction of an unrealistic phenomena known in the literature as a hydraulic drop (e.g. Reference 6).

The experimental drag force on keel # 1 in unstratified water is also shown in Figure 7. It can be seen that there is a large increase in drag for subcritical stratified flow compared to the unstratified case. In the supercritical range, the drag force for stratified flow is lower than that for unstratified flow because the stable stratification suppresses the size of the lee side recirculating region.

The values of the drag force based on hydraulic assumptions are also indicated in Figure 7. These values are significantly larger than the experimental observations, and in addition to this it can be seen that the experimental turning points in Figure 7 cannot be predicted by hydraulic theory. This is a direct result of the over simplification of the hydraulic model as compared to the two-dimensional numerical model.

The results for the drag force discussed so far are those for the shortest keel (keel # 1). Figure 8 provides the results for the drag force for keel # 4 (longest keel). The inertia of keel # 4 is too large

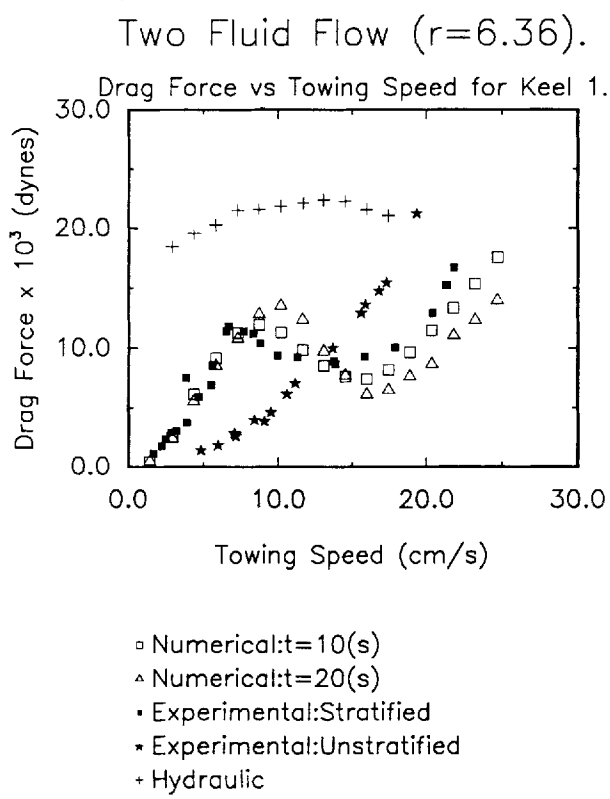

Figure 7. Drag force on keel # 1 as a function of the flow speed. ($F_0 = 1{\cdot}0$ when the upstream flow speed is 14·54 cm/s. The width of the keel is 30 cm)

to allow the experimental measurement of the drag force with reasonable accuracy, and for this keel the only data presented are those obtained through the numerical simulations. In addition to the numerical results, the drag force predictions based on hydraulic theory are also plotted. It can be seen clearly that the trends for keel # 1, as shown in Figure 7, are not all present here. The most noticeable difference in these numerical results is the absence of the second turning point (minimum) associated with the lee side recirculation. As discussed previously, it is not surprising that this feature is absent; see Figures 4 and 6. The hydraulic results follow the general trends of the numerical predictions; however, they are about twice as large. The reason for this is that, despite the mildness of the fourth keel, there is still a significant two-dimensional nature to the flow in the vicinity of the obstacle. The importance of this has been demonstrated previously for single-layer flow in plots of the lee side velocity and pressure; see, for example, Reference 13.

Further numerical studies of the lee side recirculating zone have also been undertaken; these studies looked at the effect of reducing the grid size on this vortex. It was found that reducing the grid size had no significant effect on this zone, and for all practical purposes the results were identical. In addition, computations have been made for ridges with shapes similar to the two other laboratory keels #2 and #3 in the same way as those reported here for keels #1 and #4. A review of all these results is available in a recent Ph.D. thesis by Jameel.[15]

Finally, simple skin-friction calculations have been made for a smooth flat plate and these calculations show that a plate of ≈ 70 m length is required to produce the same drag as the

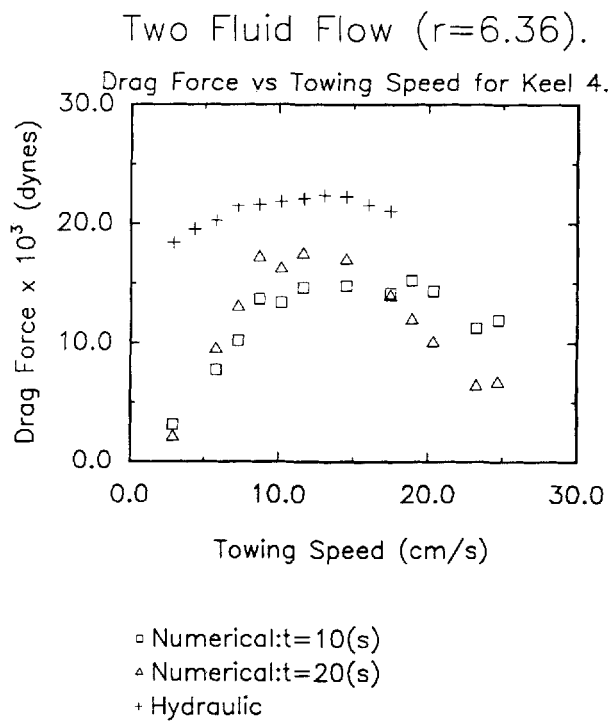

Figure 8. Drag force on keel #4 as a function of the flow speed. ($F_0 = 1{\cdot}0$ when the upstream flow speed is 14·54 cm/s. The width of the keel is 30 cm)

maximum drag found for laboratory keel #1. The typical Froude number for actual oceanic flow under real keels is normally in the range 0·2 to 0·4,[1] i.e. less than the Froude number of 0·7 for maximum drag. Depending on the spacing and distribution of ice keels, the drag force generated by these keels may be the major component of the total drag (hydrodynamic) force on the ice pack.

ACKNOWLEDGEMENTS

Financial support for this work was provided by the Natural Sciences and Engineering Research Council of Canada and the Panel on Energy Research and Development. M. I. Jameel was also awarded the Ian N. McKinnon Memorial Fellowship to complete the writing of his Ph.D. thesis.

APPENDIX: NOMENCLATURE

b_c	obstacle crest height
B_c	dimensionless obstacle height (b_c/h_0)
c	upstream bore speed
F_0	upstream Froude number
g	gravitational acceleration
h_0	upstream fluid depth of the active layer
H	total fluid depth of the two layers
r	fluid depth ratio (H/h_0)

s	fluid density ratio (ρ_2/ρ_1)
t	time
u_0	initial upstream fluid flow speed
δx	horizontal grid cell size
δy	vertical grid cell size
ρ_1	fluid density for layer #1
ρ_2	fluid density for layer #2

REFERENCES

1. D. R. Topham, H. D. Pite, D. Richards and B. Johnson, 'Stratified flows generated by an arctic ice keel', *Proc. 3rd Int. Symp. on Stratified Flow*, Pasadena, California, 1987.
2. H. D. Pite, D. R. Topham, and B. J. Van Hardenberg, 'Laboratory measurements of the drag force on two-dimensional topographic features in a two-layer flow', *J. Fluid Mech.*, (submitted for review) (1992).
3. R. R. Long, 'Some aspects of the flow of stratified fluids II. Experiments with two-fluids', *Tellus*, **6**, 97–115 (1954).
4. R. R. Long, 'Blocking effects in flow over obstacles', *Tellus*, **22**, 471–480 (1970).
5. R. R. Long, 'Some experimental observations of upstream disturbances in a two-fluid system', *Tellus*, **26**, 313–317 (1974).
6. P. G. Baines, 'A unified description of two layer flow over topography', *J. Fluid Mech.*, **146**, 127–167 (1984).
7. P. G. Baines and P. A. Davies, 'Laboratory studies of topographic effects in rotating and/or stratified fluids', *Orographic Effects in Planetary Flows*, WMO GARP Publications 23, Ch. 8, 1980.
8. D. D. Houghton and E. Isaacson, *Mountain Winds*, Study in Numerical Analysis 2, 1970, pp. 21–52.
9. D. D. Houghton and A. Kasahara, 'Non-linear shallow fluid flow over an isolated ridge', *Commun. Pure Appl. Math.*, **21**, 1–23 (1968).
10. F. H. Harlow and J. E. Welch, 'Calculation of time dependent viscous incompressible flow of fluid with free surface', *Phys. Fluids*, **8**, 2182–2189 (1965).
11. B. D. Nichols, C. W. Hirt and R. S. Hotchkiss, 'SOLA-VOF: a solution algorithm for transient fluid flow with multiple free boundaries', *Report No. LA-8355*, Los Alamos Scientific Laboratory, Los Alamos, New Mexico, 1980.
12. C. W. Hirt, 'Flow around bluff bodies', Lecture Series 1984-06, von Karman Institute for Fluid Dynamics, Belgium, 1984.
13. M. I. Jameel and R. D. Rowe, 'A numerical study of single layer flow over a ridge', *Numer. Methods Laminar Turbulent Flows*, **5**, 1362–1373 (1987).
14. C. W. Hirt, 'Introduction to numerical solution of industrial flows', Lecture Series 1986-07, von Karman Institute for Fluid Dynamics, Belgium, 1986.
15. M. I. Jameel, 'Modelling to two layer flow over an obstacle', *Ph.D. Thesis*, Department of Mechanical Engineering, The University of Calgary, 1991.